

Massive alterations of sarcoplasmic reticulum free calcium in skeletal muscle fibers lacking calsequestrin revealed by a genetically encoded probe

M. Canato^{a,1}, M. Scorzetto^{a,1}, M. Giacomello^b, F. Protasi^{c,d}, C. Reggiani^{a,d}, and G. J. M. Stienen^{e,2}

Departments of ^aHuman Anatomy and Physiology and ^bExperimental Veterinary Sciences, University of Padua, 35121 Padua, Italy; ^cCeSI, Department of Basic and Applied Medical Sciences, University G. d'Annunzio, I-66013 Chieti, Italy; ^dIIM-Interuniversity Institute of Myology and ^eLaboratory for Physiology, Institute for Cardiovascular Research, VU University Medical Center, 1081BT, Amsterdam, The Netherlands

Edited* by Clara Franzini-Armstrong, University of Pennsylvania Medical Center, Philadelphia, PA, and approved November 12, 2010 (received for review June 30, 2010)

The cytosolic free Ca^{2+} transients elicited by muscle fiber excitation are well characterized, but little is known about the free $[\text{Ca}^{2+}]$ dynamics within the sarcoplasmic reticulum (SR). A targetable ratiometric FRET-based calcium indicator (D1ER Cameleon) allowed us to investigate SR Ca^{2+} dynamics and analyze the impact of calsequestrin (CSQ) on SR $[\text{Ca}^{2+}]$ in enzymatically dissociated flexor digitorum brevis muscle fibers from WT and CSQ-KO mice lacking isoform 1 (CSQ-KO) or both isoforms [CSQ-double KO (DKO)]. At rest, free SR $[\text{Ca}^{2+}]$ did not differ between WT, CSQ-KO, and CSQ-DKO fibers. During sustained contractions, changes were rather small in WT, reflecting powerful buffering of CSQ, whereas in CSQ-KO fibers, significant drops in SR $[\text{Ca}^{2+}]$ occurred. Their amplitude increased with stimulation frequency between 1 and 60 Hz. At 60 Hz, the SR became virtually depleted of Ca^{2+} , both in CSQ-KO and CSQ-DKO fibers. In CSQ-KO fibers, cytosolic free calcium detected with Fura-2 declined during repetitive stimulation, indicating that SR calcium content was insufficient for sustained contractile activity. SR Ca^{2+} reuptake during and after stimulation trains appeared to be governed by three temporally distinct processes with rate constants of 50, 1–5, and 0.3 s^{-1} (at 26°C), reflecting activity of the SR Ca^{2+} pump and interplay of luminal and cytosolic Ca^{2+} buffers and pointing to store-operated calcium entry (SOCE). SOCE might play an essential role during muscle contractures responsible for the malignant hyperthermia-like syndrome in mice lacking CSQ.

excitation–contraction coupling | parvalbumin

Calcium ions play an important signaling role in virtually every cell type. Ca^{2+} is stored in a subcellular reticular organelle, and its release into the cytosol is triggered by action potentials and/or by second messengers, such as inositol triphosphate. In skeletal and cardiac muscle cells, Ca^{2+} is stored inside the sarcoplasmic reticulum (SR), which is in close contact with invaginations of the cell surface membrane, the T-tubular system. Action potentials propagated through the T-tubular system are sensed by the voltage sensors (dihydropyridine receptors), which are located opposite to the ryanodine receptors (RyRs), the Ca^{2+} release channels present in the terminal cisternae of the SR, and this causes calcium release (recently reviewed in 1, 2).

The transient increase in cytosolic Ca^{2+} concentration, which triggers the contractile response, has been intensively studied. Little is known about the dynamic changes of the free Ca^{2+} concentration inside the SR, however. Calsequestrin (CSQ) is an acidic high-capacity Ca^{2+} -binding protein located within the SR terminal cisternae. CSQ type 1 (CSQ1) is the major SR Ca^{2+} buffer in fast muscle fibers, whereas CSQ2 predominates in cardiomyocytes and slow muscle fibers (3, 4). CSQ serves to keep the free $[\text{Ca}^{2+}]$ low inside the SR while providing a pool of rapidly available bound calcium to maintain the free $[\text{Ca}^{2+}]$ level (5, 6). This minimizes Ca^{2+} leakage through the RyRs and reduces the dissipation of energy by the SR Ca^{2+} pump, a func-

tion essential to maintain a low metabolic rate in quiescent excitable cells. In addition, CSQ has been shown to modulate RyR-mediated Ca^{2+} release from the SR (6). To understand the pivotal role of CSQ in SR function, it is critical to determine free SR Ca^{2+} concentration, and this has been made possible by the advent of a targetable ratiometric FRET-based indicator, such as D1ER Cameleon (7). Seminal studies using this technique have been performed recently (8, 9). These studies yielded a direct estimate of 0.3 mM for free SR $[\text{Ca}^{2+}]$ (8). The magnitude of the dynamic changes in free calcium concentration proved to be small, in line with the expected calcium-buffering function of CSQ.

To understand the function of CSQ, mice carrying null mutations of the genes coding for CSQ1 or CSQ2 have been created (10, 11). Male CSQ1-null mice exhibited an increased spontaneous mortality rate and heat/halothane-induced susceptibility to trigger lethal malignant hyperthermia (MH)-like episodes (12, 13). This is indicative of perturbed calcium handling inside the cells. Contractile function in muscle fibers of CSQ1-null mice was fairly normal, however (10). To explore these findings further and to address the nature of the calcium dysregulation, we decided to measure the free $[\text{Ca}^{2+}]$ directly inside the SR of flexor digitorum brevis (FDB) muscle fibers of CSQ1-KO (CSQ-KO) mice and of CSQ1/CSQ2-null mice [i.e., CSQ-double KO (DKO) mice]. Whereas SR free $[\text{Ca}^{2+}]$ measured during quiescence was indistinguishable in fibers lacking CSQ from the value in controls, the ablation of CSQ resulted in massive changes in intraluminal calcium during electrical stimulation and in a depletion of the SR Ca^{2+} store. The large variations in SR calcium observed allowed us to characterize the kinetics of SR Ca^{2+} reuptake from the intraluminal side and to dissect three temporally well-separated components in SR Ca^{2+} reuptake, which were attributed to the activity of the SR Ca^{2+} pump and the presence of additional calcium recovery processes. This provided a clue to identify the missing link in the development of lethal muscle contractures associated with MH, which was observed in mice lacking CSQ (12).

Results

Intracellular Distribution of the Probe and CSQ Isoforms in Enzymatically Dissociated FDB Muscle Fibers. Fibers transfected with D1ER Cameleon showed a typical striation pattern (Fig. 1A) characterized by a double-sarcomeric periodicity with major

Author contributions: C.R. and G.J.M.S. designed research; M.C., M.S., M.G., C.R., and G.J.M.S. performed research; F.P. contributed new reagents/analytic tools; M.C., M.S., M.G., C.R., and G.J.M.S. analyzed data; and M.C., M.S., M.G., F.P., C.R., and G.J.M.S. wrote the paper.

The authors declare no conflict of interest.

*This Direct Submission article had a prearranged editor.

¹M.C. and M.S. contributed equally to this work.

²To whom correspondence should be addressed. E-mail: g.stienen@vumc.nl.

This article contains supporting information online at www.pnas.org/lookup/suppl/doi:10.1073/pnas.1009168108/-DCSupplemental.

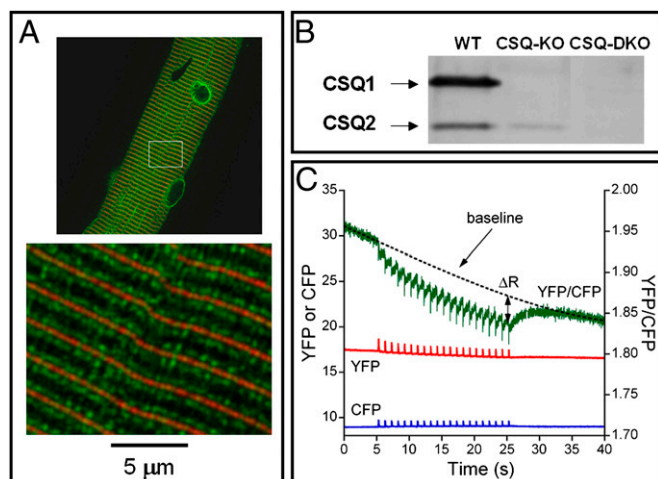


Fig. 1. (A) Localization of D1ER on both sides of Z lines stained with α -actinin antibody (D1ER, green; α -actinin antibody + rhodamine, red). Two different magnifications are shown. The sarcomere length is 2.04 μm . (B) Western blot showing the differences in expression of the two CSQ isoforms in WT, CSQ-KO, and CSQ-DKO fibers. Note the reduced expression of CSQ2 in the CSQ-KO preparation. (C) Typical recording of the SR D1ER FRET response to repetitive stimulation (20 s at 1 Hz) of a CSQ-KO muscle fiber. Stimulation started 5 s after the beginning of data acquisition ($t = 5$ s) and ended at $t = 25$ s. YFP and CFP signals (two lower traces, left ordinate) and their R (upper trace, right ordinate), measures of the free SR Ca^{2+} concentration, are shown. The YFP/CFP R values during the initial and final intervals of 5 s were used to calculate the baseline, which is indicated by the interrupted line. The ΔR (double-sided arrow) reflects the decrease in the SR Ca^{2+} concentration during the train of stimuli.

localizations on both sides of the Z lines visualized with an antibody specific to α -actinin. Such a pattern is similar to that of CSQ or other SR proteins in the terminal cisternae (14), thus confirming the localization of D1ER in the SR (9). Some thin connections crossing the Z lines were detectable, however, suggesting the presence of the probe in the longitudinal component of the SR. This pattern was consistently present in WT, CSQ-KO, and CSQ-DKO fibers (Fig. S1). In WT FDB muscle, CSQ1 was more abundant than CSQ2 (Fig. 1B), in accordance with data showing that slow fibers represent less than 20% of the whole FDB fiber population (15, 16). As expected only CSQ2 was observed in CSQ1-null muscles and both isoforms were lacking in CSQ1-CSQ2 null muscles. In agreement with previous observations, CSQ2 was down-regulated in CSQ1-null mice (10).

SR Free $[\text{Ca}^{2+}]$ in Quiescent Fibers. Free intra-SR Ca^{2+} concentration was derived from the ratio (R) of the YFP and CFP intensities. The initial recordings from the first fiber examined in each Petri dish were used to determine the basal values of the YFP/CFP ratios to eliminate any possible effect of electrical stimulation and bleaching of the calcium sensor. The basal values were derived from the intercept at time 0 of a linear fit of the R during the first 5 s of data collection before starting electrical stimulation (Fig. 1C). The average R values were 1.75 ± 0.05 , 1.86 ± 0.04 , and 1.84 ± 0.03 in WT ($n = 26$), CSQ-KO ($n = 25$), and CSQ-DKO ($n = 21$) fibers, respectively, with no significant difference between the groups (ANOVA).

Changes in SR Free $[\text{Ca}^{2+}]$ During Electrical Stimulation. Representative examples of variations of R values during contractions elicited by trains of electrical stimulation at 1, 5, 20, and 60 Hz in fibers from WT and CSQ-DKO animals are shown in Figs. 1C and 2. A striking difference can be noticed between WT and CSQ-DKO fibers. In WT fibers, only minor changes in the R,

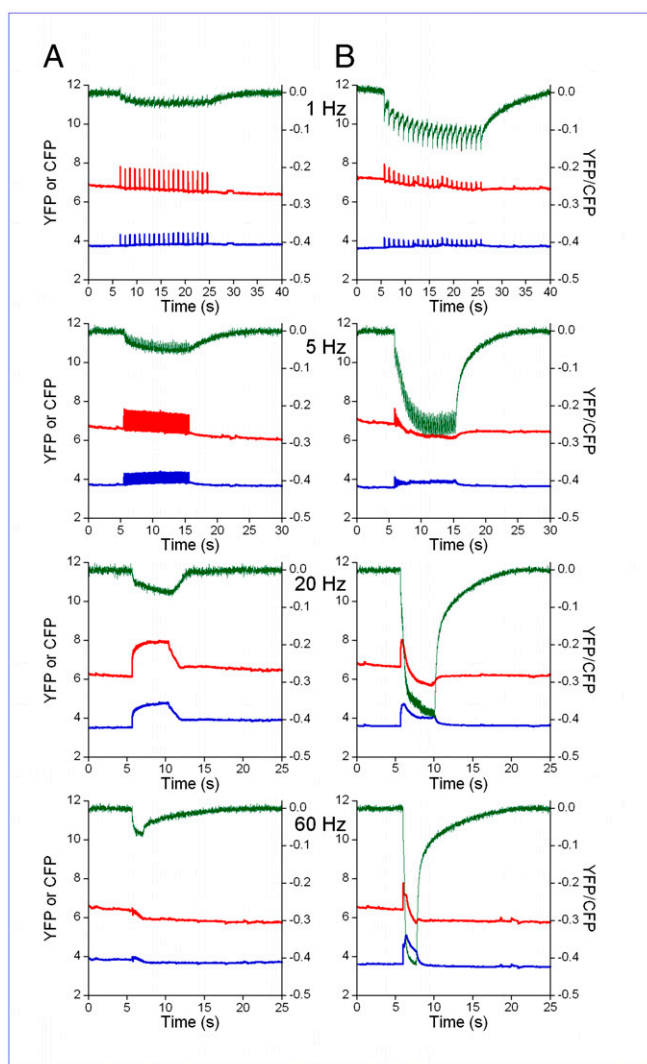


Fig. 2. Typical recordings of changes in intraluminal SR Ca^{2+} concentrations during repetitive stimulation at different stimulation rates. The D1ER responses (YFP, red; CFP, blue; YFP/CFP R, green) are shown in a WT fiber (A) and a CSQ-KO fiber (B) at 1, 5, 20, and 60 Hz. The R signal has been corrected for the alterations in baseline as described in the text. Note the striking difference between WT and CSQ-KO in the amplitude of the changes in the R related to contractile activity. Resting R values obtained for the fibers shown in A are 1.83 (1 Hz), 1.81 (5 Hz), 1.78 (20 Hz), and 1.70 (60 Hz), and those for the fibers shown in B are 2.00 (1 Hz), 1.95 (5 Hz), 1.88 (20 Hz), and 1.81 (60 Hz).

and thus in SR free $[\text{Ca}^{2+}]$, were observed during repetitive electrical stimulation, whereas in CSQ-DKO fibers, large drops in SR free $[\text{Ca}^{2+}]$ occurred with every single twitch at 1 Hz and became even more pronounced during tetanic stimulation at 60 Hz. The overall reduction in SR free $[\text{Ca}^{2+}]$ during the train of stimuli was quantified by the drop in the R at the end of the train of stimuli (ΔR), after correction for bleaching. Although the average ΔR was small and showed only a minor increase with stimulation frequency in WT fibers, the decrease in SR calcium concentration was much larger than in WT in CSQ-KO and CSQ-DKO fibers, with no significant differences between CSQ-KO and CSQ-DKO fibers (Fig. 3). Interestingly, an increase in stimulation rate from 20 to 60 Hz caused only a minor increase in the ΔR . This observation, as well as the similarity between the value of the R reached at the end of 60-Hz trains and that reached in depletion experiments (Fig. S2), suggests that in the

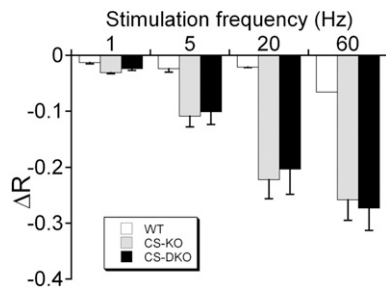


Fig. 3. Average amplitudes of the decline in the YFP/CFP R (ΔR) during contractile activity with increasing stimulation frequency. The decrease in the R in fibers from WT, CSQ-KO, and CSQ-DKO reflects the decrease in the SR Ca^{2+} concentration at the end of the trains of stimuli. The decrease is small and remains rather constant in WT fibers at the stimulation frequencies used but increases markedly in both KO groups.

absence of CSQ, the SR was almost depleted of calcium during high-frequency trains.

Kinetics of SR Refilling. The large reductions in SR free $[\text{Ca}^{2+}]$ provided a unique occasion to analyze the time course of Ca^{2+} reuptake into the SR viewed from the luminal side. Importantly, the time course of the R recovery after the end of a train of stimuli depended on the amplitude of the decline of the R (ΔR) during the train (i.e., on the level of depletion of the SR Ca^{2+}).

In WT fibers at all stimulation frequencies, in CSQ-KO and CSQ-DKO fibers at 1 Hz, and in very few CSQ-KO and CSQ-DKO fibers at higher frequencies, recovery at the end of a train of stimulation was dominated by a single exponential with a rate constant (k) of $\approx 0.3 \text{ s}^{-1}$ (Table 1). In other cases (i.e., in CSQ-KO and CSQ-DKO fibers at 5, 20, and 60 Hz), recovery followed a double-exponential time course (as illustrated in Fig. 4A). The slower rate constant in these cases (k_s) was close to 0.3 s^{-1} ; hence, it was similar to the rate constant dominating the monoexponential recovery (k). The rate of the faster process (k_f) ranged between 2.7 and 5.4 s^{-1} . Interestingly, the amplitude of the slow phase (a_s) remained constant, whereas the amplitude of the fast phase (a_f) increased with the frequency of stimulation. These results clearly show that SR refilling is governed by (at least) two processes with rate constants differing by an order of magnitude and that the faster process is detectable only when large drops in the R (i.e., in SR free $[\text{Ca}^{2+}]$) occur and only in fibers lacking CSQ.

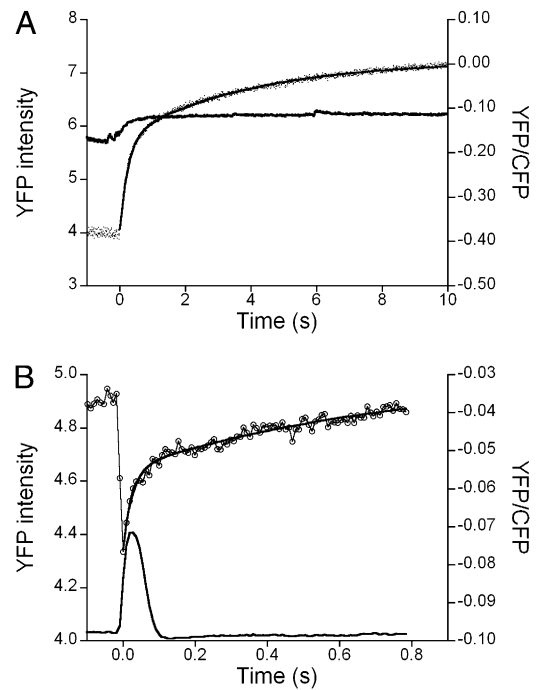


Fig. 4. Time course of the change in the YFP/CFP R during the SR refilling. (A) Time course of the increase in the YFP/CFP R after a train of stimuli at 60 Hz in a CSQ-KO fiber. (B) Time course of the variations in the YFP/CFP R during a train of stimuli at 1 Hz in a CSQ-KO fiber. YFP signal is shown as a surrogate marker of mechanical activity. In A, the rise in YFP intensity marks the onset of relaxation. In B, the YFP intensity reflects the twitch time course of the fiber. In A and B, a double exponential was fitted to the YFP/CFP data points. The parameter values in A are $a_f = 0.21$, $k_f = 4.20 \text{ s}^{-1}$, $a_s = 0.18$, and $k_s = 0.26 \text{ s}^{-1}$, and those in B are $b_f = 0.021$, $m_f = 44.1 \text{ s}^{-1}$, $b_s = 0.025$, and $m_s = 1.36 \text{ s}^{-1}$.

In individual twitches during a train of stimulation at low frequency (1 Hz), calcium reuptake took place at an even faster rate than the fastest rate resolved after the end of the stimulation train. This early phase of calcium reuptake into the SR was quantified from the time-averaged records during the final 10 twitches of the 1-Hz stimulation train. A representative example of these recordings is shown in Fig. 4B. Two rate constants

Table 1. Parameters of the exponential equations interpolating the recovery of the R expressing intraluminal SR free Ca^{2+} concentration at the end of the trains of stimuli at different stimulation frequencies

Hz	Type	ΔR	n	$k, \text{ s}^{-1}$	n	a_f	$k_f, \text{ s}^{-1}$	a_s	$k_s, \text{ s}^{-1}$	n
1	WT	0.013 ± 0.002	19	0.277 ± 0.021	18	—	—	—	—	—
	CSQ-KO	0.031 ± 0.002	38	0.329 ± 0.023	28	—	—	—	—	—
	CSQ-DKO	0.024 ± 0.003	23	0.354 ± 0.024	23	—	—	—	—	—
5	WT	0.024 ± 0.006	6	0.254 ± 0.026	5	—	—	—	—	—
	CSQ-KO	0.109 ± 0.019	8	0.294	1	0.040 ± 0.007	2.810 ± 0.441	0.069 ± 0.014	0.268 ± 0.018	7
	CSQ-DKO	0.101 ± 0.023	9	0.291 ± 0.029	3	0.066 ± 0.012	2.686 ± 0.105	0.076 ± 0.009	0.288 ± 0.012	6
20	WT	0.021 ± 0.001	2	0.208	1	—	—	—	—	—
	CSQ-KO	0.222 ± 0.034	7	0.343	1	$0.128 \pm 0.025^*$	$4.136 \pm 0.211^*$	0.100 ± 0.017	0.291 ± 0.010	6
	CSQ-DKO	0.203 ± 0.045	9	0.231	1	$0.148 \pm 0.027^*$	$4.061 \pm 0.197^*$	0.090 ± 0.010	0.279 ± 0.011	7
60	WT	0.066	1	0.205	1	—	—	—	—	—
	CSQ-KO	0.258 ± 0.037	6	—	—	$0.136 \pm 0.030^*$	$5.389 \pm 1.039^*$	0.093 ± 0.013	0.247 ± 0.034	6
	CSQ-DKO	0.273 ± 0.040	7	—	—	$0.190 \pm 0.032^*$	$4.066 \pm 0.595^*$	0.091 ± 0.013	0.201 ± 0.046	7

The R signal obtained after baseline subtraction was fitted to a single exponential with recovery rate k and to a double-exponential $R = a_f \exp(-k_f t) + a_s \exp(-k_s t)$, in which a_f and a_s and k_f and k_s denote the amplitudes and rates of the fast and slow components, respectively. When the amplitude of the recovery process (ΔR) was small, a single exponential provided an adequate fit. For larger amplitudes, a double exponential was required and was sufficient to provide an adequate fit. Note that the rate constant describing the slow component of the double exponential is similar to the monoexponential rate constant.

(m_f and m_s) governing the early phase with amplitudes b_f and b_s were derived from a double-exponential fit to the averaged data points from each fiber (Table S1). The amplitudes and rate constants in CSQ-KO and CSQ-DKO were similar, with the rate constant of the faster component being close to 50 s^{-1} and the rate constant of slower component being $\approx 1 \text{ s}^{-1}$.

Cytosolic Free Ca^{2+} Transients During and After Repetitive Stimulation. To assess whether the SR depletion had an impact on the cytosolic calcium transients, we determined cytosolic free $[\text{Ca}^{2+}]$ with the fluorescent indicator Fura-2 acetoxyethyl ester (AM). At rest, cytosolic free $[\text{Ca}^{2+}]$ was not significantly different in WT and CSQ-DKO fibers (fluorescence R of WT: 0.87 ± 0.05 , fluorescence R of CSQ-DKO: 0.92 ± 0.04), whereas a marked difference in the calcium transients was detectable during repetitive stimulations at 1, 5, 20, and 60 Hz (Fig. 5 and Fig. S34). In CSQ-DKO fibers, a marked decline followed the initial peak in calcium concentration reached during stimulation, whereas in WT fibers, free $[\text{Ca}^{2+}]$ rose after the first stimulus and then stabilized during the maintained stimulation. The rate of decline in the free calcium level during stimulation increased with a stimulation frequency up to 4 s^{-1} as shown in Fig. S3B.

The change in cytosolic $[\text{Ca}^{2+}]$ corresponding to SR refilling was studied by interpolating the decline of the peak Fura-2 signals with exponential equations. The time course of the decay of the fluorescence R in a single twitch at a 1-Hz stimulation rate was described by a single exponential, with a rate constant of $17.2 \pm 3.2 \text{ s}^{-1}$ in WT fibers and $20.1 \pm 3.0 \text{ s}^{-1}$ in CSQ-DKO fibers. The decay at the end of a train of repeated stimulations was interpolated with a double-exponential curve, and the parameters are reported in Table S2. The first fast phase of the decline in cytosolic calcium concentration was characterized by a rate constant (n_f) of about 18 s^{-1} , whereas the second slow phase was characterized by a rate constant (n_s) of about 0.7 s^{-1} , without significant differences between WT and CSQ-DKO fibers. Differences in amplitude between WT and CSQ-DKO fibers were present in the first fast phase but not in the second slow phase of decay.

Discussion

The key findings of the present study are as follows: (i) the SR free $[\text{Ca}^{2+}]$ values at rest in WT, CSQ-KO, and CSQ-DKO fibers were not significantly different; (ii) a massive decrease in intraluminal free SR calcium concentration was observed during repeated stimulation in CSQ-KO and CSQ-DKO fibers, leading to depletion of SR and decline of the cytosolic free $[\text{Ca}^{2+}]$; and (iii) the large reductions in intraluminal SR Ca^{2+} in CSQ-KO and CSQ-DKO fibers provided unique insights into the kinetics of SR refilling with high time resolution.

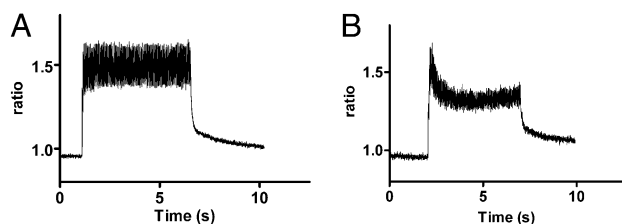


Fig. 5. Fibers lacking CSQ are not able to maintain a high cytosolic calcium concentration during repetitive stimulations. Typical recordings of cytosolic Ca^{2+} concentrations visualized by the Fura-2 fluorescence R in a WT fiber (A) and CSQ-DKO fiber (B) during repetitive stimulation at 20 Hz are shown. Note the striking difference between WT and CSQ-DKO in the ability to maintain a high cytosolic calcium concentration during high-frequency repetitive stimulation.

SR Free $[\text{Ca}^{2+}]$ at Rest in WT, CSQ-KO, and CSQ-DKO Fibers. The basal SR free $[\text{Ca}^{2+}]$ during quiescence was not significantly different in the presence or absence of CSQ. This is in line with the notion that intraluminal concentration at rest is mainly determined by the balance between calcium reuptake and leakage (5, 17, 18). Our results thus suggest that the SR free $[\text{Ca}^{2+}]$ at rest does not depend on the buffering power provided by CSQ.

The resting SR $[\text{Ca}^{2+}]$ calculated on the basis of the affinity of the SR calcium probe ranged between 0.2 and 0.5 mM (SI Materials and Methods). It should be noted that a K_d value of 0.2 mM [as calculated by Rudolf et al. (8)] implies that the probe would be almost saturated in quiescent fibers, however, and this implies that even a small increase in the R could reflect a considerable increase in resting $[\text{Ca}^{2+}]$. Thus, our results do not rule out the possibility that SR free $[\text{Ca}^{2+}]$ might reach 0.8 mM in CSQ-KO fibers, as suggested by Murphy et al. (5) from a reanalysis of data published by Paolini et al. (10).

Fluctuations of SR Free $[\text{Ca}^{2+}]$ with Contractions in CSQ-KO and CSQ-DKO Fibers. The free SR $[\text{Ca}^{2+}]$ changes associated with electrical stimulation were small in control fibers, whereas massive alterations were observed in the CSQ-KO and CSQ-DKO fibers. Evidence was obtained indicating that the SR in CSQ-KO and CSQ-DKO fibers could be virtually depleted during repetitive electrical stimulation. The Fura-2 measurements indicated that this depletion of the SR was accompanied by the inability to sustain the cytosolic free calcium level during contraction (Fig. 5B). Because the time-averaged cytosolic free calcium concentration increased with stimulation frequency, such a decline in the Fura-2 signal is compatible with the presence of a cytosolic calcium buffer with an equilibration rate constant of $\approx 4 \text{ s}^{-1}$, similar to k_{off} of parvalbumin for Mg^{2+} (19). This suggests that part of the calcium released from the SR was scavenged by parvalbumin and that depletion of the SR Ca^{2+} store prevented maintenance of the initial peak of free $[\text{Ca}^{2+}]$. The reductions in the amplitudes of the YFP and CFP signals, which are surrogate markers of the contractile activity of the fibers, indicate that this decline was accompanied by a depression of the contractile response, and thus in the amount calcium bound to troponin C (Fig. 2).

To maintain the high cytosolic free $[\text{Ca}^{2+}]$ during a tetanic contraction, the high-affinity sites on troponin C ($80 \mu\text{M} \times 2$), the SR Ca^{2+} pump ($120 \mu\text{M} \times 2$), and parvalbumin ($430 \mu\text{M} \times 2$) need to be saturated. A drop in the cytosolic free $[\text{Ca}^{2+}]$ to less than 50% of its peak value associated with the binding of calcium to parvalbumin and virtually complete depletion of the SR implies that not more than 600–700 $\mu\text{mol/L}$ muscle fiber can be released with repeated stimulations from the SR in muscle fibers lacking CSQ. This is agreement with the reduced calcium content of SR previously shown in CSQ-KO (10) and CSQ-DKO (20) fibers.

Processes Governing SR Calcium Refilling. The analysis of the recovery of the R from the drop that corresponds to calcium release induced by a single action potential or a train of action potentials revealed that SR refilling was governed by three distinct processes. An early rapid process with a rate of $\approx 50 \text{ s}^{-1}$, a process with an intermediate rate ranging between 2.7 and 5.4 s^{-1} , and a relatively slow process with a rate of about 0.3 s^{-1} could be identified. Importantly, both the amplitude and rate of the intermediate process depended strongly on stimulation frequency or amplitude of the decrease in the R (and in SR free $[\text{Ca}^{2+}]$) during the train of stimuli. Although the contribution of intraluminal calcium buffers other than CSQ cannot be excluded (discussed in 5, 20), the kinetics of the recovery of SR free $[\text{Ca}^{2+}]$ can be described according to a model based on distinct refilling processes as outlined below.

- i. The fast process: Comparison with the time course of the contractile twitch response indicates that the fast process at

least partly coincides with the decline in cytosolic free Ca^{2+} below the threshold of force generation (Fig. 4B). This process is likely related to calcium reuptake via the SR Ca^{2+} pump. Model descriptions of the pump kinetics in FDB fibers are available and provide values $\geq 30 \text{ s}^{-1}$ (21, 22). D1ER is a rapid calcium sensor with a $k_{\text{on}} = 3.6 \times 10^6 \text{ M}^{-1} \cdot \text{s}^{-1}$ and a $k_{\text{off}} = 256 \text{ s}^{-1}$ (7). This indicates that the rate constants estimated from our recordings are not limited by the characteristics of the probe. In contrast, Fura-2 is a slow calcium sensor with a k_{off} close to 26 s^{-1} (23), thus close to the rate constant for the fast process on the cytosolic side.

- ii. The intermediate process: This process can be detected when the SR calcium concentration is quite low. The amplitude and rate constant of the intermediate process were clearly discernible only in CSQ-KO and CSQ-DKO fibers and increased with stimulation frequency and/or amplitude of the decrease in the R during the train of stimuli (i.e., with the level of depletion of the SR). To the best of our knowledge, there is no evidence for stimulation frequency-dependent inactivation of the SR calcium reuptake process. Thus, it appears that this component of SR calcium reuptake depends on the actual free calcium concentration inside the SR and is present only when the SR is virtually empty. This unique feature of the calcium restitution process could be resolved in the present experiments because the powerful buffering of the luminal free $[\text{Ca}^{2+}]$ usually provided by CSQ was absent. The exact nature of this process remains to be established. Because this component of SR refilling is not detectable in the cytosol, possible candidates or contributors should be searched for in mitochondrial calcium efflux (24) or extracellularly. In this latter case, refilling via store-operated calcium entry (SOCE) (25) might be invoked. Fura-2 experiments performed in the absence of external calcium (Fig. S4) reveal that proper function of CSQ-DKO fibers relies on the presence of external calcium, a finding consistent with SOCE. A recent study (26) on fibers in which CSQ expression was down-regulated by shRNA-I arrived at a similar conclusion.
- iii. The slow process: This process of SR refilling with a rate constant of about 0.3 s^{-1} was evident not only in CSQ-KO and CSQ-DKO fibers but in WT fibers. This slow process likely corresponds to the “tail” of the cytosolic calcium transient, as described in frog (27) and mouse (28) muscle fibers. Evidence suggests that this process is related to the reuptake of calcium that was bound to parvalbumin in the cytosol, whose concentration amounts to 0.43 mM (29). Yet unidentified buffers in the cytosol or in the SR lumen might be involved as well, however.

The reported value for the calcium-off rate of parvalbumin is $\sim 1 \text{ s}^{-1}$ (19), and thus very close to the measured rate constant. This interpretation of the slow component is supported by the decline in peak cytosolic calcium transient measured during and after the train of stimuli using Fura-2. The cytosolic free calcium decreases exponentially during subsequent stimuli because cytosolic calcium binds to parvalbumin by replacing magnesium, a process limited by the Mg-off rate constant of 4 s^{-1} . When the cytosolic $[\text{Ca}^{2+}]$ decreases to basal levels after the train of stimuli, this calcium is pumped back into the SR at a rate limited by the calcium-off rate of parvalbumin (1 s^{-1}).

It is worth noting that the presence of a luminal buffer other than CSQ (as mentioned above) could also influence the kinetics of the changes in free SR $[\text{Ca}^{2+}]$. The effect of such additional buffering would be a slowing of the luminal transport from the sites of calcium uptake toward the sites of calcium release and the addition of a component determined by the speed of equil-

ibration of the calcium-free and calcium-bound forms. Even if the k_{on} of calcium binding were fast, the speed of the initial (fast) phases of the refilling process might be influenced.

Conclusions and Implications

The genetically encoded ratiometric calcium probe D1ER allowed us to measure the free Ca^{2+} concentration inside the SR directly and to study Ca^{2+} reuptake into the SR from the luminal side. This led us to identify a unique intermediate component in the SR Ca^{2+} reuptake process.

The observation that sustained tetanic contractions in CSQ-KO and CSQ-DKO are blunted by cytosolic calcium buffering seems at variance with the strong contractures that are, in fact, typical of the MH-like syndrome observed in mice lacking CSQ (12). Because the SR is virtually emptied by ordinary tetanic contractions, the large amount of calcium required for a prolonged contraction cannot be provided by an intracellular store. The dramatic loss of the contractile response of fibers lacking CSQ exposed to calcium-free medium points to the relevance of extracellular calcium. We therefore propose that contractures are supported by calcium coming from extracellular space and that store-operated channels, activated by the SR depletion reached after a short tetanus, are the most likely candidates responsible for an extra component of the SR refilling process. Accordingly, SOCE might be the missing link in the explanation of the devastating contractions seen in the syndrome of MH.

Materials and Methods

An expanded discussion of materials and methods is provided in [SI Materials and Methods](#).

D1ER Expression in Adult Muscle Fibers. D1ER Cameleon in pcDNA3 (kindly donated by R.Y. Tsien, University of California, San Diego, CA) was used in transfection experiments. FDB muscles were transfected *in vivo* as described previously (30). Seven days after transfection, mice were killed by cervical dislocation, their muscles were rapidly dissected, and single fibers were isolated according to a previously described collagenase treatment (31).

Immunocytochemistry and Western Blotting. Fixed fibers were incubated with primary antibody specific for α -actinin (Sigma) and with fluorescent secondary antibody (Alexa Fluor 568 Anti-mouse; Invitrogen). The fibers were viewed with a confocal microscope (VICO; Nikon). CSQ expression was determined by SDS gel electrophoresis and Western blotting as described previously (10).

Intra-SR Calcium Detection with D1ER. Fibers bathed with imaging buffer at $25\text{--}26 \text{ }^\circ\text{C}$ were initially stimulated with a train (20-s duration) at 1 Hz, followed by stimulation trains at higher frequency. SR free calcium levels were monitored using an inverted fluorescence microscope (Eclipse-Ti; Nikon Instruments). The excitation wavelength was 435 nm (10-nm bandwidth). YFP and CFP intensities were recorded by means of a cooled CCD camera (C9100-13; Hamamatsu) equipped with a 515-nm dichroic mirror at 535 nm (40-nm bandwidth) and 480 nm (30-nm bandwidth), respectively.

Cytosolic Calcium Determination with Fura-2 AM. Fibers were loaded with $5 \mu\text{M}$ Fura-2 AM (Molecular Probes, Invitrogen) as described previously (10). After a minimum of 30 min, calcium signals were recorded using a dual-beam excitation fluorescence photometry setup (IonOptix Corp.) at $25 \text{ }^\circ\text{C}$. Calibration of the Fura-2 signals and calculation of free cytosolic calcium concentration are reported in [SI Materials and Methods](#).

ACKNOWLEDGMENTS. We thank Paul D. Allen and Bjorn C. Knollmann for the generation of CSQ1/CSQ2-null mice. We thank Drs. C. Paolini and M. Dainese (University G. d'Annunzio, Chieti, Italy) for providing the animals used in the experiments. We thank Luana Toniolo and Nicky Boontje for their help with Western immunoblotting and data analysis, respectively. This study was supported by Grant GGP08153 from the Italian Telethon Foundation (to F.P. and C.R.) and by Research Funds from the University G. d'Annunzio (to F.P.).

- Dulhunty AF (2006) Excitation-contraction coupling from the 1950s into the new millennium. *Clin Exp Pharmacol Physiol* 33:763–772.
- Rossi AE, Dirksen RT (2006) Sarcoplasmic reticulum: The dynamic calcium governor of muscle. *Muscle Nerve* 33:715–731.
- Sacchetto R, Volpe P, Damiani E, Margreth A (1993) Postnatal development of rabbit fast-twitch skeletal muscle: Accumulation, isoform transition and fibre distribution of calsequestrin. *J Muscle Res Cell Motil* 14:646–653.
- Beard NA, Laver DR, Dulhunty AF (2004) Calsequestrin and the calcium release channel of skeletal and cardiac muscle. *Prog Biophys Mol Biol* 85:33–69.
- Murphy RM, Larkins NT, Mollica JP, Beard NA, Lamb GD (2009) Calsequestrin content and SERCA determine normal and maximal Ca^{2+} storage levels in sarcoplasmic reticulum of fast- and slow-twitch fibres of rat. *J Physiol* 587:443–460.
- Royer L, Rios E (2009) Deconstructing calsequestrin. Complex buffering in the calcium store of skeletal muscle. *J Physiol* 587:3101–3111.
- Palmer AE, Jin C, Reed JC, Tsien RY (2004) Bcl-2-mediated alterations in endoplasmic reticulum Ca^{2+} analyzed with an improved genetically encoded fluorescent sensor. *Proc Natl Acad Sci USA* 101:17404–17409.
- Rudolf R, Magalhães PJ, Pozzan T (2006) Direct in vivo monitoring of sarcoplasmic reticulum Ca^{2+} and cytosolic cAMP dynamics in mouse skeletal muscle. *J Cell Biol* 173:187–193.
- Jiménez-Moreno R, Wang ZM, Messi ML, Delbono O (2010) Sarcoplasmic reticulum Ca^{2+} depletion in adult skeletal muscle fibres measured with the biosensor D1ER. *Pflugers Arch* 459:725–735.
- Paolini C, et al. (2007) Reorganized stores and impaired calcium handling in skeletal muscle of mice lacking calsequestrin-1. *J Physiol* 583:767–784.
- Knollmann BC, et al. (2006) Casq2 deletion causes sarcoplasmic reticulum volume increase, premature Ca^{2+} release, and catecholaminergic polymorphic ventricular tachycardia. *J Clin Invest* 116:2510–2520.
- Dainese M, et al. (2009) Anesthetic- and heat-induced sudden death in calsequestrin-1-knockout mice. *FASEB J* 23:1710–1720.
- Protasi F, Paolini C, Dainese M (2009) Calsequestrin-1: A new candidate gene for malignant hyperthermia and exertional/environmental heat stroke. *J Physiol* 587:3095–3100.
- Franzini-Armstrong C, Protasi F, Ramesh V (1998) Comparative ultrastructure of Ca^{2+} release units in skeletal and cardiac muscle. *Ann N Y Acad Sci* 853:20–30.
- Bruton JD, et al. (2010) Increased fatigue resistance linked to Ca^{2+} -stimulated mitochondrial biogenesis in muscle fibres of cold-acclimated mice. *J Physiol* 588:4275–4288.
- Gonzalez E, Messi ML, Zheng Z, Delbono O (2003) Insulin-like growth factor-1 prevents age-related decrease in specific force and intracellular Ca^{2+} in single intact muscle fibres from transgenic mice. *J Physiol* 552:833–844.
- Fryer MW, Stephenson DG (1996) Total and sarcoplasmic reticulum calcium contents of skinned fibres from rat skeletal muscle. *J Physiol* 493:357–370.
- Launikonis BS, et al. (2005) Confocal imaging of $[\text{Ca}^{2+}]_i$ in cellular organelles by SEER, shifted excitation and emission ratioing of fluorescence. *J Physiol* 567:523–543.
- Hou TT, Johnson JD, Rall JA (1991) Parvalbumin content and Ca^{2+} and Mg^{2+} dissociation rates correlated with changes in relaxation rate of frog muscle fibres. *J Physiol* 441:285–304.
- Royer L, et al. (2010) Paradoxical buffering of calcium by calsequestrin demonstrated for the calcium store of skeletal muscle. *J Gen Physiol* 136:325–338.
- Westerblad H, Allen DG (1994) Relaxation, $[\text{Ca}^{2+}]_i$ and $[\text{Mg}^{2+}]_i$ during prolonged tetanic stimulation of intact, single fibres from mouse skeletal muscle. *J Physiol* 480:31–43.
- Westerblad H, Allen DG (1994) The role of sarcoplasmic reticulum in relaxation of mouse muscle; effects of 2,5-di(tert-butyl)-1,4-benzohydroquinone. *J Physiol* 474:291–301.
- Baylor SM, Hollingworth S (1988) Fura-2 calcium transients in frog skeletal muscle fibres. *J Physiol* 403:151–192.
- Rudolf R, Mongillo M, Magalhães PJ, Pozzan T (2004) In vivo monitoring of Ca^{2+} uptake into mitochondria of mouse skeletal muscle during contraction. *J Cell Biol* 166:527–536.
- Dirksen RT (2009) Checking your SOCCs and feet: The molecular mechanisms of Ca^{2+} entry in skeletal muscle. *J Physiol* 587:3139–3147.
- Zhao X, et al. (2010) Increased store-operated Ca^{2+} entry in skeletal muscle with reduced calsequestrin-1 expression. *Biophys J* 99:1556–1564.
- Klein MG, Kovacs L, Simon BJ, Schneider MF (1991) Decline of myoplasmic Ca^{2+} , recovery of calcium release and sarcoplasmic Ca^{2+} pump properties in frog skeletal muscle. *J Physiol* 441:639–671.
- Westerblad H, Allen DG (1992) Myoplasmic free Mg^{2+} concentration during repetitive stimulation of single fibres from mouse skeletal muscle. *J Physiol* 453:413–434.
- Westerblad H, Allen DG (1991) Changes of myoplasmic calcium concentration during fatigue in single mouse muscle fibers. *J Gen Physiol* 98:615–635.
- DiFranco M, Quinonez M, Capote J, Vergara J (2009) DNA transfection of mammalian skeletal muscles using in vivo electroporation. *J Vis Exp* 32:1520.
- Defranchi E, et al. (2005) Imaging and elasticity measurements of the sarcolemma of fully differentiated skeletal muscle fibres. *Microsc Res Tech* 67:27–35.

Supporting Information

Canato et al. 10.1073/pnas.1009168108

SI Materials and Methods

Animals. Experiments were carried out on 4-mo-old CSQ1-null, CSQ1/CSQ2-null, and WT mice. Only male mice were used in view of the pronounced gender diversity reported in CSQ1-null mice (1). CSQ1-null mice were obtained as previously described (2). CSQ1/CSQ2-null mice were kindly provided by Paul D. Allen (Brigham and Women's Hospital, Harvard University Medical School, Boston, MA) and were generated by crossing CSQ1-null mice with CSQ2-null mice kindly provided by Bjorn Knollmann (Departments of Medicine and Pharmacology, Vanderbilt University School of Medicine, Nashville, TN) (3). WT C57BL/6J mice (same strain as KO mice) were purchased from the Charles River Laboratories. The use of the animals and the experimental protocol were approved by the ethical committee and by the animal welfare coordinator of the Department of Anatomy and Physiology, University of Padova. Mice were maintained in an accredited animal house and examined daily.

Transfection. D1ER Cameleon in pcDNA3 (kindly donated by R.Y. Tsien, University of California, San Diego, CA) was used in transfection experiments. The structural and functional characterization of D1ER is reported by Palmer et al. (4). FDB muscles were transfected in vivo as described by DiFranco et al. (5). Briefly, before electroporation, $\approx 10 \mu\text{L}$ of 2 mg/mL hyaluronidase (type IV from bovine testes; Sigma-Aldrich) was injected s.c. near the FDB muscles to improve transfection efficiency. One hour later, 15 μg of cDNA diluted in sterile physiological solution was injected. After 10 min, the muscles were electroporated by applying 20 pulses (1 Hz, 20-ms duration, 100-V/cm field strength) between two s.c. electrodes. Seven days after transfection, mice were killed by cervical dislocation, their muscles were rapidly dissected, and single fibers were isolated.

Isolation and Culture of Adult Muscle Fibers. Enzymatic isolation of single skeletal muscle fibers was performed using collagenase treatment as described by Defranchi et al. (6). Isolated cells were seeded on laminin-coated coverslips and left to adhere and stabilize overnight in tissue culture medium at 36 °C. The next morning, the coverslips were mounted in a measuring chamber containing imaging buffer (composition: 125 mM NaCl, 5 mM KCl, 1 mM CaCl_2 , 1 mM MgSO_4 , 1 mM KH_2PO_4 , 5 mM glucose, 20 mM HEPES) and equipped with platinum field electrodes. Temperature during the measurements was kept at 25–26 °C to slow the kinetics of calcium release and reuptake into the SR and to facilitate comparison with previous studies.

Immunocytochemistry. Fibers were fixed with 4% (vol/vol) formalin in PBS for 30 min, permeabilized with 1% Triton, and blocked in 10% (vol/vol) goat serum for 1 h to avoid nonspecific signal. Fibers were incubated with primary antibody specific for α -actinin (Sigma) overnight at 4 °C; after three washes (20 min each), they were incubated with fluorescent secondary antibodies (Alexa Fluor 568 Anti-mouse; Invitrogen) for 2 h at room temperature. The fibers were viewed with a confocal microscope (VICO; Nikon).

Western Blotting. CSQ expression in FDB homogenates and single fibers was determined by SDS gel electrophoresis and Western blotting as described previously (2). Proteins were separated on 10% (vol/vol) SDS-polyacrylamide gel and transferred to nitrocellulose. Immunostaining of blots was performed using rabbit polyclonal antibody reactive with both isoforms of CSQ (Affinity Bioreagents)

and anti-rabbit alkaline phosphatase-conjugated antibody (Sigma). An ECL protocol was used for visualization of bands.

Intra-SR Calcium Detection with D1ER. Fibers prepared as described above and bathed with imaging buffer were initially stimulated with a train (20-s duration) of bipolar stimuli at 1 Hz with an amplitude of 20 V and a duration of 1 ms. Fiber illumination and data collection started 5 s before the beginning of stimulation and ended 15 s after the end of stimulation; hence, they lasted a total of 40 s (Fig. 1C). Recordings were usually obtained from two to five fibers in the same Petri dish; thereafter, a final series of recordings was obtained in one fiber at stimulation frequencies of 5, 20, and 60 Hz with corresponding durations of 10, 5, and 2 s, respectively.

SR free calcium levels were monitored using an inverted fluorescence microscope (Eclipse-Ti; Nikon Instruments) equipped with the perfect focus system (PFS; Nikon Instruments). The measuring chamber was mounted onto a movable plate to position the fibers optimally in the field of view of the inverted microscope (Eclipse Ti). Excitation of the fluorophore was performed by means of an Hg arc lamp (100 W; Nikon) using a 435-nm filter (10-nm bandwidth). YFP and CFP intensities were recorded by means of a cooled CCD camera (C9100-13; Hamamatsu) equipped with a 515-nm dichroic mirror at 535 nm (40-nm bandwidth) and 480 nm (30-nm bandwidth), respectively. Two images of 256 \times 128 pixels each were collected with an integration time of the camera of 8 ms by means of a simultaneous dual-channel imaging system (OES). Image processing and storage with the 12-bit frame grabber typically occurred in 1 ms, resulting in a time resolution of 9 ms. In some fibers, the time resolution during the experiments was increased to 4 ms by collecting images at one-quarter of the original size. To reduce noise in this latter case, excitation intensity was also increased by a factor of 4 by removing the 0.25 neutral density filter present in the excitation path, resulting in faster "bleaching" of the calcium sensor.

YFP and CFP intensities were corrected for background by defining two corresponding regions of interest (ROIs) in each channel: one relatively large ROI containing part of the fiber, taking care that the fiber segment selected remained within the ROI during the contractions, and a smaller ROI located near the border of the image for background recording. Care was taken to select in both the YFP and the CFP image-corresponding regions of the fiber and background. The R was defined as follows:

$$R = (\text{YFP}_{\text{fiber}} - \text{YFP}_{\text{background}}) / (\text{CFP}_{\text{fiber}} - \text{CFP}_{\text{background}})$$

As can be seen in Fig. 1C, bleaching caused a slight decrease in the YFP signal and a minor increase in the CFP signal. This is an intrinsic feature of FRET-based probes, because bleaching of the acceptor leads to an increase in donor fluorescence. These opposite changes lead to a progressive slow decrease of the YFP/CFP R during the period of data acquisition. Correction for the change in baseline during the experiment was performed by fitting a third-order polynomial through the initial and final 5-s periods at the beginning and end of the recordings. The polynomial was subsequently subtracted from the recordings to remove time-dependent changes in the baseline and allow determination of the stimulation-dependent changes in the R (indicated as ΔR) and the measurement of their amplitude and time course. In Fig. 1C, it should be noted that the YFP and CFP signals increased to some extent during contraction as the fiber shortened and more sarcomeres entered the ROI. The ratiometric nature of the cal-

cium sensor accounts for such movement artifacts; however, the amplitude and time course of the changes in the individual YFP and CFP signals could be used as surrogate markers of contractile activity of fibers. It is worth noting that the alignment of the camera and choice of the ROI are critical and may lead to movement artifacts. The area scanned by the digital camera was divided by the dichroic mirror into two equal rectangular regions used, respectively, for the YFP signal and the CFP signal. The alignment of the camera is limited by the pixel size of the image obtained. Careful inspection of the recording showed that the maximum movement artifact in the recordings of the YFP/CFP ratio (R) amounted to 0.05, with an average value close to 0.02.

Details related to the calibration of the D1ER calcium sensor are reported below.

Cytosolic Calcium Determination with Fura-2 AM. Fibers were loaded with 5 μM Fura-2 AM (Molecular Probes, Invitrogen) in incubation buffer (2), washed twice for 10 min with incubation buffer without BSA at 37 °C to retain the indicator in the cytosol, and immersed in imaging buffer. After a minimum of 30 min, calcium signals were recorded using a dual-beam excitation fluorescence photometry setup (IonOptix Corp.) at 25 °C. Fibers were stimulated following the same protocol described above for intrasr Ca^{2+} determination. $[\text{Ca}^{2+}]_i$ measurements were expressed as fluorescence R of the emission at 480 nm with reference to the excitation wavelengths of 360 and 380 nm, respectively. Calibration of the Fura-2 signals and calculation of the free cytosolic calcium concentration are reported below.

Statistical Analysis. Data are expressed as the mean \pm SEM. Comparisons between groups were made using two-way ANOVA, followed by a Bonferroni post hoc test. $P < 0.05$ was considered statistically significant. Polynomial and exponential curve fitting was performed using Kaleidagraph 3.5 (Synergy Software).

SI Results

Intracellular Distribution of the Probe in WT, CSQ-KO, and CSQ-DKO Muscle Fibers. The fluorescence patterns of FDB fibers transfected with D1ER Cameleon are shown in Fig. S1. As can be seen, D1ER (green) is localized on both sides of the Z line, as revealed by immunostaining with anti- α -actinin antibody (red). The same pattern is present in all three types of fibers, regardless of the presence of CSQ. The densitometric scanning of the calcium-independent D1ER fluorescence along the major axis of the fiber shows two closer peaks for each sarcomere, with an average interval of 0.64 μm and a sarcomeric periodicity of about 1.95 μm .

Calibration of the D1ER Calcium Sensor and Calculation of SR Free Calcium Concentrations. Calibration of the calcium sensor was performed as described (7, 8). The minimum value of the R (R_{\min}) was determined as is illustrated in Fig. S2. In these experiments, integration time of the CCD camera was increased to 360 ms and excitation intensity was decreased accordingly to avoid saturation of the camera. As a result, bleaching was negligible during these experiments.

Butanedione monoxime (BDM; 20-mM final concentration) was added to reduce possible movement artifacts. Subsequently, the SR Ca^{2+} pump was inhibited by cyclopiazonic acid (CPA) dissolved in DMSO (20- μM final concentration of CPA, 1% final concentration of DMSO) to prevent calcium reuptake into the SR during the experiment. On CPA addition in CSQ-KO fibers as in this example, the R started to decrease slightly, reflecting slow calcium leak from the SR, which is balanced by calcium reuptake under steady-state conditions in the absence of CPA. Three minutes later, ionomycin (Iono) was added as indicated in the figure (final concentrations indicated). In most experiments, 4 μM Iono proved to be sufficient to reach R_{\min} . The average

levels reached in four fibers were: $R_{\min} = 1.58 \pm 0.04$ with $\Delta R = R - R_{\min} = 0.415 \pm 0.031$, where the R is the basal initial value.

During the SR calcium measurements, the R occasionally reached lower values than the R_{\min} . This may be attributed to bleaching of the probe. Experiments were performed to assess R_{\min} in the presence of the bleaching, which usually occurred during a series of measurements wherein the frequency dependence of the change in SR calcium concentration was assessed. In these experiments, the fiber was continuously illuminated for 40 + 30 + 25 + 25 s = 120 s, before the determination of R_{\min} as described above. The ΔR obtained in this experiment was very similar to the ΔR obtained in unbleached fibers. This suggests that bleaching mainly affects the baseline of the R value and not the sensitivity of the calcium sensor per se.

As also noted (8, 9), determination of R_{\max} in muscle cells is not straightforward because cells contract at high Ca^{2+} even in the presence of BDM or N-benzyl-p-toluene sulfonamide (BTS). Close inspection of the recordings shown in Fig. 2 after the application of 5 mM calcium indicated a value for R_{\max} of at least 1.9. The highest R values of recorded ranged between 2.2 and 2.4. The actual free SR $[\text{Ca}^{2+}]$ value could be estimated using the classic equation, $[\text{Ca}^{2+}] = \beta \cdot K'_d \cdot [(R - R_{\min}) / (R_{\max} - R)]^{1/n}$, proposed by Grynkiewicz et al. (10). Assuming an apparent K_d (K'_d) of 200 μM as calculated by Rudolf et al. (8), a β -value of 1.5 derived from the R of emission of YFP at 480 nm (11), a Hill coefficient (n) of 1.67 (4), the R_{\min} value given above, and the R_{\max} value taken as the highest R value observed under our experimental conditions, the resting calcium concentration will be 0.18 mM at $R = 1.75$ or 0.55 mM at $R = 1.85$.

Calibration of the Fura-2 Signal and Calculation of Cytosolic Free Calcium Concentrations. Muscle fiber fluorescence R was converted to free cytosolic calcium concentration $[\text{Ca}^{2+}]_{\text{CY}}$ using the equation $[\text{Ca}^{2+}]_{\text{CY}} = (R - R_{\min}) / (R_{\max} - R) \cdot K_D \cdot \beta$, where R is the ratio of fluorescence excited at 340 nm to that excited at 380 nm and K_D is the affinity constant of Fura-2 for calcium, which was taken at 145 nM (Molecular Probes). R_{\min} and R_{\max} were determined in Iono-permeabilized myofibers: R_{\min} was the minimum R value measured in calcium-free solution, and R_{\max} was the maximal R value measured in 2 mM calcium solution. β was derived as the F380 calcium-free/F380 calcium-saturated R from previously published data (12). Under these assumptions, the resting cytosolic calcium concentration will be 71 nM at $R = 0.87$ and 87 nM at $R = 0.92$.

Decline of Fura-2 Signal/Cytosolic Calcium with Repetitive Stimulation. Fig. S3 shows two series of calcium transients during stimulation trains at 1, 5, 20, and 60 Hz recorded in WT and CSQ-DKO fibers, respectively. A striking difference between WT and CSQ-DKO in the ability to maintain a high cytosolic calcium concentration during repetitive stimulation can be seen in Fig. S3A. The amplitude of the response to the first stimuli increases with the stimulation rate in both WT and CSQ-DKO fibers, whereas the decay of the fluorescence R on repetitive stimulation is present only in CSQ-DKO fibers and becomes more pronounced with the stimulation rate and with the number of stimuli delivered (20 stimuli at 1 Hz, 50 stimuli at 5 Hz, 100 stimuli at 20 Hz, and 120 stimuli at 60 Hz). The rate constant of the decline of Fura-2 fluorescence signal during repetitive stimulation increases as a function of stimulation rate, reaching a maximum of $\approx 4 \text{ s}^{-1}$ (Fig. S3B).

Decline of Fura-2 Signal/Cytosolic Calcium in CSQ-DKO Fibers in 0 Calcium. To test whether SOCE might be involved in the maintenance of contraction in KO fibers, Fura-2 responses in WT and CSQ-DKO fibers were recorded in the absence of external calcium, by immersing the fibers in a buffer in which 1 mM CaCl_2 was omitted and 50 μM EGTA was added to scavenge trace

amounts of calcium (Fig. S4). The WT fibers appeared to function normally, but the amplitude of the Fura-2 transients

decayed rapidly in CSQ-DKO fibers. This behavior is consistent with the SOCE hypothesis.

1. Dainese M, et al. (2009) Anesthetic- and heat-induced sudden death in calsequestrin-1-knockout mice. *FASEB J* 23:1710–1720.
2. Paolini C, et al. (2007) Reorganized stores and impaired calcium handling in skeletal muscle of mice lacking calsequestrin-1. *J Physiol* 583:767–784.
3. Knollmann BC, et al. (2006) Casq2 deletion causes sarcoplasmic reticulum volume increase, premature Ca²⁺ release, and catecholaminergic polymorphic ventricular tachycardia. *J Clin Invest* 116:2510–2520.
4. Palmer AE, Jin C, Reed JC, Tsien RY (2004) Bcl-2-mediated alterations in endoplasmic reticulum Ca²⁺ analyzed with an improved genetically encoded fluorescent sensor. *Proc Natl Acad Sci USA* 101:17404–17409.
5. DiFranco M, Quinonez M, Capote J, Vergara J (2009) DNA transfection of mammalian skeletal muscles using in vivo electroporation. *J Vis Exp* 32:1520.
6. Defranchi E, et al. (2005) Imaging and elasticity measurements of the sarcolemma of fully differentiated skeletal muscle fibres. *Microsc Res Tech* 67:27–35.
7. Palmer AE, Tsien RY (2006) Measuring calcium signaling using genetically targetable fluorescent indicators. *Nat Protoc* 1:1057–1065.
8. Rudolf R, Magalhães PJ, Pozzan T (2006) Direct in vivo monitoring of sarcoplasmic reticulum Ca²⁺ and cytosolic cAMP dynamics in mouse skeletal muscle. *J Cell Biol* 173:187–193.
9. Jiménez-Moreno R, Wang ZM, Messi ML, Delbono O (2010) Sarcoplasmic reticulum Ca²⁺ depletion in adult skeletal muscle fibres measured with the biosensor D1ER. *Pflugers Arch* 459:725–735.
10. Grynkiewicz G, Poenie M, Tsien RY (1985) A new generation of Ca²⁺ indicators with greatly improved fluorescence properties. *J Biol Chem* 260:3440–3450.
11. Miyawaki A, Griesbeck O, Heim R, Tsien RY (1999) Dynamic and quantitative Ca²⁺ measurements using improved cameleons. *Proc Natl Acad Sci USA* 96:2135–2140.
12. Fraysse B, et al. (2006) Fiber type-related changes in rat skeletal muscle calcium homeostasis during aging and restoration by growth hormone. *Neurobiol Dis* 21:372–380.

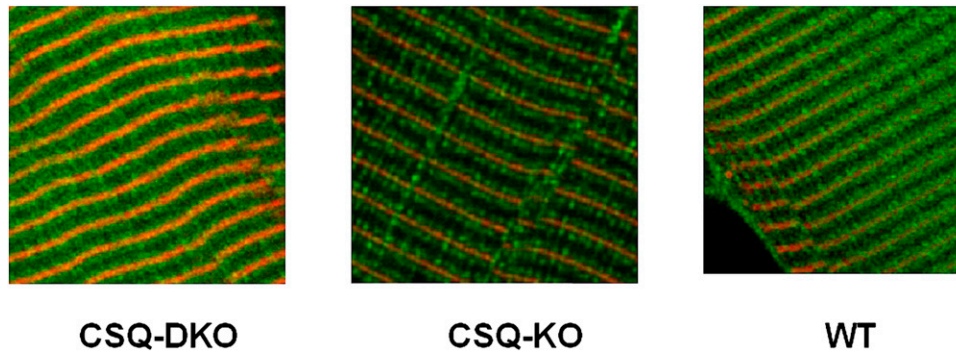


Fig. S1. Localization of D1ER in WT, CSQ-KO, and CSQ-DKO fibers. In all cases, D1ER is localized on both sides of Z lines stained with anti- α -actinin antibody (D1ER, green; anti- α -actinin antibody + rhodamine, red). Sarcomere lengths are 1.92 μm (CSQ-DKO), 1.96 μm (CSQ-KO), and 1.91 μm (WT).

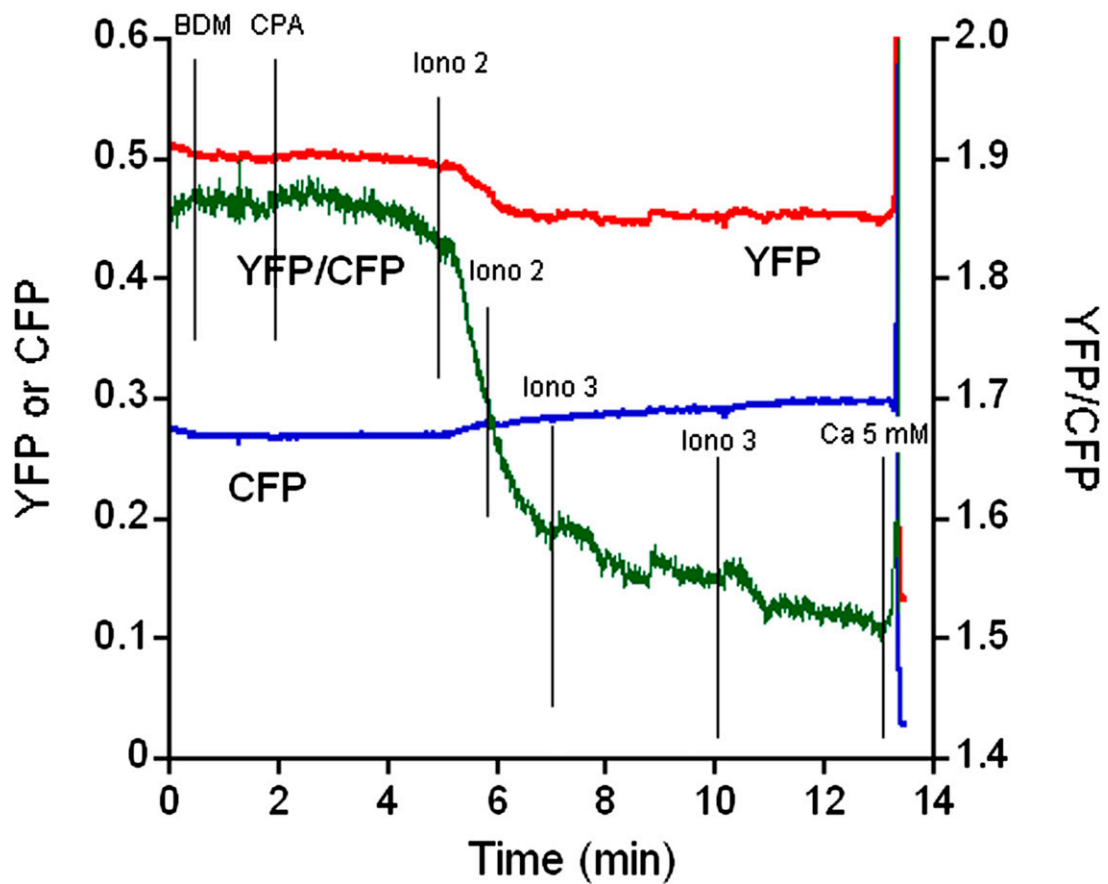


Fig. S2. Calibration of D1ER. The experimental protocol used for calibration of the D1ER Cameleon Ca^{2+} sensor is shown. First, 20 mM butanedione monoxime (BDM) was added to prevent movement artifacts. Subsequently, the SR Ca^{2+} pump was inhibited by addition of 20 μM CPA to prevent calcium reuptake into the SR during the experiment. On CPA addition in CSQ-KO fibers, as in this example, the R started to decrease slightly, reflecting slow Ca^{2+} leak from the SR. Subsequently, aliquots of ionomycin (Iono) were added (concentrations indicated in μM), causing a progressive decrease in the R. After a plateau was reached, 5 mM CaCl_2 was added, which caused an abrupt increase in YFP (red), CFP (blue), and R (green) signals but also contraction of the fiber, which moved out of focus.

Table S1. Amplitudes and rate constants of the recovery of the R expression of the SR Ca²⁺ concentration after a single twitch during a train at a stimulation rate of 1 Hz

	b_f	m_f, s^{-1}	b_s	m_s, s^{-1}	n
WT	0.010	39.3	0.044	0.19	1
CSQ-KO	0.018 ± 0.001	47.2 ± 5.6	0.040 ± 0.006	1.05 ± 0.09	6
CSQ-DKO	0.019 ± 0.002	52.1 ± 6.7	0.058 ± 0.009	0.95 ± 0.21	4

The R signal obtained after baseline subtraction was fitted to a double-exponential $R = b_f \exp(-m_f t) + b_s \exp(-m_s t)$, in which b_f and b_s and m_f and m_s denote the amplitudes and rates of the fast and slow components, respectively.

Table S2. Amplitudes and rate constants of the decline phase of the free cytosolic Ca²⁺ concentration as detected by the Fura-2 fluorescence R at the end of the trains at different stimulation frequencies

Hz	Type	n	c_f	n_f, s^{-1}	c_s	n_s, s^{-1}	c
1	WT	55	0.37 ± 0.06	19.8 ± 3.1	0.06 ± 0.01	1.3 ± 0.3	0.84 ± 0.02
	CSQ-DKO	45	0.36 ± 0.04	18.7 ± 0.8	0.08 ± 0.02	1.6 ± 0.7	0.88 ± 0.01
5	WT	55	0.32 ± 0.03	19.7 ± 3.5	0.09 ± 0.01	1.2 ± 0.3	0.85 ± 0.02
	CSQ-DKO	45	0.28 ± 0.05	17.8 ± 1.3	0.09 ± 0.01	0.8 ± 0.1	0.88 ± 0.01
20	WT	55	0.33 ± 0.03	19.5 ± 5.3	0.15 ± 0.06	1.3 ± 0.6	0.85 ± 0.06
	CSQ-DKO	45	0.18 ± 0.10	13.7 ± 6.7	0.10 ± 0.01	0.7 ± 0.4	0.90 ± 0.09
60	WT	55	0.35 ± 0.09	26.0 ± 9.4	0.16 ± 0.01	1.1 ± 0.1	0.84 ± 0.03

The fluorescence R signals were fitted to a double-exponential $R = c_f \exp(-n_f t) + c_s \exp(-n_s t) + c$, in which c_f and c_s and n_f and n_s denote the amplitudes and rates of the fast and slow components, respectively. No reliable parameters could be obtained for the transients at 60 Hz in CSQ-DKO fibers because of the decay of Fura-2 signals during the stimulation train.